# Synthesis, Structural Characterization, and Reactivity Studies of 5-CF$_3$SO$_3$-B$_{10}$H$_{13}$

Emily R. Berkeley, William C. Ewing, Patrick J. Carroll, and Larry G. Sneddon*

Department of Chemistry, University of Pennsylvania, Philadelphia, Pennsylvania 19104-6323, United States

Ⓢ *Supporting Information*

ABSTRACT: In contrast to previous reactions carried out in cyclopentane solvent at room temperature that produced 6-TfO-B$_{10}$H$_{13}$ (TfO = CF$_3$SO$_3$), the reaction of *closo*-B$_{10}$H$_{10}^{2-}$ with a large excess of trifluoromethanesulfonic acid in the ionic liquid 1-butyl-3-methylimidazolium trifluoromethanesulfonate (bmimOTf) gave exclusively the previously unknown 5-TfO-B$_{10}$H$_{13}$ isomer. Experimental and computational studies demonstrated that the difference in the products of the two reactions is a result of 6-TfO-B$_{10}$H$_{13}$ isomerizing to 5-TfO-B$_{10}$H$_{13}$ above room temperature in bmimOTf solutions. Reactivity studies showed that 5-TfO-B$_{10}$H$_{13}$: (1) is deprotonated by reaction with 1,8-bis(dimethylamino)-naphthalene to form the 5-TfO-B$_{10}$H$_{12}^{1-}$ anion; (2) reacts with alcohols to produce 6-RO-B$_{10}$H$_{13}$ boryl ethers (R = Me and 4-CH$_3$O-C$_6$H$_4$); (3) undergoes olefin-hydroboration reactions to

form 5-TfO-6,9-R$_2$-B$_{10}$H$_{11}$ derivatives; and (4) forms a 5-TfO-6,9-(Me$_2$S)$_2$-B$_{10}$H$_{11}$ adduct at its Lewis acidic 6,9-borons upon reaction with dimethylsulfide. The 5-TfO-6,9-(Me$_2$S)$_2$-B$_{10}$H$_{11}$ adduct was also found to undergo alkyne-insertion reactions to form a range of previously unreported triflate-substituted 4-TfO-*ortho*-carboranes (1-R-4-TfO-1,2-C$_2$B$_{10}$H$_{10}$) and reactions with triethylamine or ammonia to form the first TfO-substituted decaborate [R$_3$NH$^+$]$_2$[2-TfO-B$_{10}$H$_9^{2-}$], and [R$_3$NH$^+$]$_2$[1-TfO-B$_{10}$H$_9^{2-}$] (R = H, Et) salts.
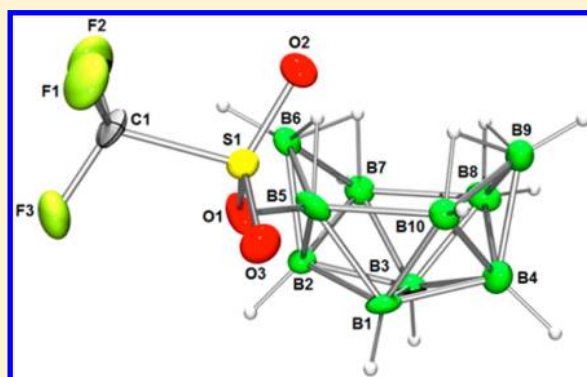
The previously reported[1] synthesis of [Et$_3$NH$^+$]$_2$[*closo*-B$_{10}$H$_{10}^{2-}$] from the readily available and safe-to-handle [Et$_3$NH$^+$][BH$_4^-$] salt makes the *closo*-B$_{10}$H$_{10}^{2-}$ decaborate anion[2] a potentially attractive alternative to B$_{10}$H$_{14}$ as a starting material for the syntheses of the larger-cage polyboranes that are needed for many technological and/or medical applications.[3] Several recently reported studies have yielded significant advances toward realizing this potential.[4−7]

Hawthorne showed that *closo*-B$_{10}$H$_{10}^{2-}$ undergoes a cage-opening reaction to form 6-R-B$_{10}$H$_{13}$ (R = Ph, Cy, TfO (TfO = CF$_3$SO$_3$)) compounds when reacted with benzene, cyclohexane (eq 1), or triflate ion (eq 2) in the presence of trifluoromethanesulfonic (triflic) acid (HOTf).[4] Crystallographic
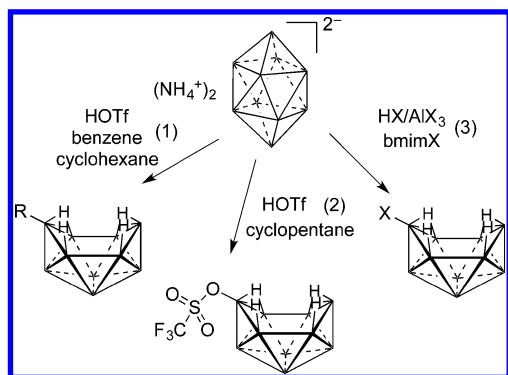
studies confirmed the exclusive formation of the 6-R-B$_{10}$H$_{13}$ isomers. The hydroxyl-derivative 6-HO-B$_{10}$H$_{13}$ was similarly synthesized from B$_{10}$H$_{10}^{2-}$ upon reaction with sulfuric acid in hexanes.[5] Ewing demonstrated[6] (eq 3) the high-yield syntheses of the 6-X-B$_{10}$H$_{13}$ (X = Cl, Br, I) halo-decaboranes by the cage-opening reactions of *closo*-B$_{10}$H$_{10}^{2-}$ with super acidic mixtures of HX (X = Cl, Br) and an aluminum halide in the ionic liquids bmimCl, bmimBr, and bmimI (bmim = 1-butyl-3-methylimidazolium). It was then further shown[7] that each 6-X-B$_{10}$H$_{13}$ could be converted to its 5-X-B$_{10}$H$_{13}$ isomer by a base-catalyzed isomerization reaction.

Even with these recent developments, new methods are still needed to enable the efficient conversion of the closed-cage framework of *closo*-B$_{10}$H$_{10}^{2-}$ to a wider range of polyboranes and functionalized polyborane derivatives. In this Paper, we demonstrate that, in contrast to the triflic acid reaction reported by Hawthorne, when the cage opening of *closo*-B$_{10}$H$_{10}^{2-}$ with triflic acid is carried out at 60 °C in a bmimOTf/HOTf solution, only the 5-TfO-B$_{10}$H$_{13}$ isomer is formed. Reactivity studies of 5-TfO-B$_{10}$H$_{13}$ are also presented demonstrating that this compound and its derivatives can be converted to a range of useful polyboranes and carboranes.

■ EXPERIMENTAL SECTION

General Procedures. Unless otherwise noted, all reactions and manipulations were performed in dry glassware under nitrogen atmospheres using the high-vacuum or inert-atmosphere techniques described by Shriver and Drezdzon.[8]

Materials. Phenylacetylene, trifluoromethylphenylacetylene, 3-phenyl-1-propyne, *tert*-butyl propiolate, cyclohexylacetylene, 1,8-nonadiyne, 1-octyne, propargyl acetate, and 4-bromo-1-butyne (Sigma-Aldrich) were used as received. 6-TfO-$B_{10}H_{13}$,[4] 6,9-$(Me_2S)_2$-$B_{10}H_{12}$,[9] 5-I-$B_{10}H_{13}$,[7] and $[NH_4^+]_2[closo$-$B_{10}H_{10}^{2-}]$[10] were prepared as previously described. The bmimOTf (Fluka) was azeotropically dried by refluxing with toluene, followed by high-vacuum drying at 100 °C and then storage in a N_2-filled drybox. High-performance liquid chromatography (HPLC)- or American Chemical Society (ACS)-grade hexanes, triethylamine, pentane, ether, dichloromethane, dimethylsulfide, triflic acid, 1,8-bis(dimethylamino)-naphthalene (Proton Sponge, PS), and silica gel (Fischer, 230−400 mesh) were used as received. C_6D_6 (D, 99.5%), $CDCl_3$ (D, 99.9%), and CD_2Cl_2 (D, 99.9%) (Cambridge Isotope) were used as received. Toluene (Fisher) was dried over sodium prior to use.

Physical Measurements. ^1H NMR spectra at 400.1 MHz and ^{11}B NMR spectra at 128.4 MHz were obtained on a Bruker DMX 400 spectrometer. All ^{11}B NMR chemical shifts are referenced to external $BF_3 \cdot OEt_2$ (0.00 ppm), with a negative sign indicating an upfield shift. All ^1H chemical shifts were measured relative to residual protons in the lock solvents and are referenced to Me_4Si (0.00 ppm). High- and low-resolution mass spectra (HRMS and LRMS) using negative chemical ionization (NCI) or electrospray ionization (ESI) techniques were recorded on a Micromass Autospec Spectrometer or Waters GC-TOF Premier, respectively. Infrared (IR) spectra were recorded on a PerkinElmer Spectrum 100 FT-IR spectrometer using NaCl plates. Elemental analyses were performed at the Microanalytical Laboratory, UC Berkeley. Melting points (mp) were obtained on a standard melting-point apparatus and are uncorrected.

5-TfO-$B_{10}H_{13}$ (1). Method A. Triflic acid (5.8 mL, 65.0 mmol) was added dropwise to a rapidly stirring solution of $[NH_4^+]_2[closo$-$B_{10}H_{10}^{2-}]$ (1.0 g, 6.5 mmol) in bmimOTf (3 mL, 8.05 mmol), and the solution was heated at 60 °C for 12 h. The mixture was extracted with hexanes (∼300 mL) until ^{11}B NMR analysis showed the extracts contained no product. The extracts were filtered to remove any solids, and the solvent was vacuum-evaporated to give an off-white viscous liquid. Two recrystallizations from pentane produced a white solid.

For **1**: 1.14 g (4.2 mmol, 64%), mp 28−29 °C. ^{11}B NMR (128.4 MHz, $CDCl_3$) (int, mult, J_{BH} = Hz) 12.3 (1, d, 154), 11.6 (2, d, br), 9.3 (1, s), 7.3 (1, d, 157), 2.4 (1, d, 153), −0.2 (1, d, 173), −4.8 (1, d, 161), −36.5 (1, d, 106), −37.2 (1, d, 113) ppm. Density functional theory/gauge-independent atomic orbital (DFT/GIAO)-calculated ^{11}B NMR shifts (assign) 13.3 (B3), 12.4 (B1), 8.6 (B5), 7.7 (B9), 4.5 (B6), 3.1 (B10), −1.1 (B8), −4.5 (B7), −39.7 (B4), −39.7 (B2) ppm. $^1H\{^{11}B\}$ NMR (400.1 MHz, $CDCl_3$) (int, assign) 4.1 (1, BH), 4.0 (2, BH), 3.8 (1, BH), 3.3 (1, BH), 3.2 (1, BH), 3.1 (1, BH), 1.2 (1, BH), 0.7 (1, BH), 0.4 (1, BH), −1.5 (1, BH), −1.8 (1, BH), −2.0 (1, BH) ppm. NCI HRMS: *m/z* calc for $CH_{13}B_{10}O_3F_3S$: 272.1482, found: 272.1468. Anal. Calcd: C: 4.44, H: 4.85; found: C: 4.54, H: 4.94. IR (NaCl, cm^{-1}): 3584 (w), 2591 (s), 1901 (w), 1509 (m), 1400 (s), 1219 (s), 1147 (s), 1096 (s), 1037 (m), 995 (s), 953 (m), 875 (m), 622 (s). Crystals of **1** suitable for a crystallographic determination were obtained by slow evaporation of a hexanes solution.

Method B: Thermal Isomerization in bmimOTf. 6-TfO-$B_{10}H_{13}$ (50 mg, 0.19 mmol) was stirred in bmimOTf (1 mL) or bmimOTf/HOTf at 55 °C for 36 h. The observed 5-TfO-$B_{10}H_{13}$ products were extracted from the bmimOTf solutions with pentane, and the pentane was then vacuum-evaporated to give 39 mg (0.15 mmol, 78%) and 34 mg (0.13 mmol, 68%) of **1**, respectively.

Method C: Thermal Isomerization in Toluene. When 6-TfO-$B_{10}H_{13}$ (50 mg, 0.19 mmol) was stirred in toluene (5 mL) at 55 °C, no reaction was observed after 30 h; however, when it was stirred at 85 °C for 36 h, ^{11}B NMR analysis showed complete conversion to **1**. The toluene was vacuum-evaporated to give 46 mg (0.17 mmol, 92%) of **1**.

Method D: Base Isomerization. 6-TfO-$B_{10}H_{13}$ (100 mg, 0.37 mmol) was reacted with 3 μL (0.02 mmol) of triethylamine in toluene (5 mL) at room temperature for 1 h. Toluene and triethylamine were vacuum-evaporated to give 70 mg (0.26 mmol, 70%) of **1**.

[PSH$^+$][5-TfO-$B_{10}H_{12}^-$] (1$^-$). A mixture of **1** (40 mg, 0.15 mmol) and Proton Sponge (PS) (31.7 mg, 0.15 mmol) was reacted in $CDCl_3$ (1 mL) at room temperature for 24 h. On the basis of NMR analysis, **1$^-$** was produced in 95% yield.

For **1$^-$**: yellow oil. ^{11}B NMR (128.4 MHz, CH_2Cl) (int, mult, J_{BH} = Hz) 11.6 (1, d, br), 10.1 (1, s), −3.0 (1, d, 138), −9.0 (1, d, ∼117), −11.4 (1, d, 144), −12.9 (1, d, br), −14.4 (1, d, ∼159), −16.8 (1, d, 138), −34.2 (1, d, 148), −49.3 (1, d, 149) ppm. DFT/GIAO-calculated ^{11}B NMR shifts (assign) 16.4 (B6), 15.4 (B5), 6.3 (B1), −5.8 (B8), −6.6 (B3), −9.3 (B10), −13.6 (B7), −13.9 (B9), −29.8 (B2), −47.5 (B4) ppm. $^1H\{^{11}B\}$ NMR (400.1 MHz, $CDCl_3$) (int, assign) 8.72 (1, PS$^+$-NHN), 7.69−7.97 (6, CH), 3.96 (1, BH), 3.19 (12, $4CH_3$), 2.86 (1, BH), 2.80 (2, BH), 2.58 (1, BH), 2.37 (2, BH), 0.71 (1, BH), 0.14 (1, BH, br), −2.47 (1, BH, br), −3.08 (1, BH, br) ppm (the remaining BH resonance was not resolvable). ESI (neg) HRMS: *m/z* calc for $CH_{12}B_{10}O_3F_3S$: 271.1390, found: 271.3192. IR (NaCl, cm^{-1}): 3207 (m), 2961 (w), 2540 (s), 1463 (m), 1370 (s), 1264 (s), 1201 (s), 1157 (s), 1098 (m), 1031 (s), 980 (s), 912 (m), 859 (w), 831 (m), 767 (s), 733 (m), 638 (s).

6-CH_3O-$B_{10}H_{13}$ (2). A mixture of **1** (100 mg, 0.37 mmol) and methanol (30 mg, 0.93 mmol) was stirred at 70 °C in dichloroethane for 20 h. After the solvent was vacuum-evaporated, the remaining solid was extracted with pentane. The pentane was vacuum-evaporated to give **2** (45.0 mg, 0.30 mmol, 80%) as a white solid. The ^{11}B and ^1H NMR spectra of **2** were consistent with those previously reported.[11]

6-(4-CH_3O-C_6H_4O)-$B_{10}H_{13}$ (3). A mixture of **1** (100 mg, 0.37 mmol) and 4-methoxyphenol (50 mg, 0.40 mmol) was stirred at 70 °C in dichloroethane for 20 h. After the solvent was vacuum-evaporated, the remaining solid was extracted with pentane. The pentane was vacuum-evaporated to give **3** as a white solid.

For **3**: 69.1 mg, (0.31 mmol, 84%), mp 168−170 °C. ^{11}B NMR (128.4 MHz, CH_2Cl) (int, mult, J_{BH} = Hz) 22.1 (1, s), 3.2 (3, d, 154), 1.4 (2, d, 155), −15.1 (2, d, 161), −33.8 (1, d, 147), −44.8 (1, d, 137) ppm. $^1H\{^{11}B\}$ NMR (400.1 MHz, CD_2Cl_2) (int, assign) 6.85−7.26 (4, C_6H_4), 3.85 (1, BH), 3.79 (3, CH_3), 3.27 (2, BH), 3.19 (2, BH), 2.23 (2, BH), 0.27 (2, BH), −0.36 (2, BH, br), −1.77 (2, BH, br) ppm. NCI HRMS: *m/z* calc for $C_7H_{20}B_{10}O_2$: 246.2394, found: 246.2402. IR (NaCl, cm^{-1}): 3223 (s), 2835 (w), 2579 (w), 2259 (w), 1632 (w), 1605 (w), 1510 (s), 1441 (m), 1366 (m), 1298 (w), 1230 (s), 1180 (m), 1102 (m), 1032 (m), 825 (s), 733 (s), 459 (m).

5-TfO-6,9-$(C_5H_{11})_2$-$B_{10}H_{11}$ (4) and 5-I-6,9-$(C_5H_{11})_2$-$B_{10}H_{11}$ (5). In separate reactions, a mixture of **1** (150 mg, 0.55 mmol) and $PtBr_2$ (20 mol %, 39.0 mg, 0.11 mmol) and a mixture 5-I-$B_{10}H_{13}$ (100 mg, 0.39 mmol) and $PtBr_2$ (20 mol %, 27.7 mg, 0.08 mmol) were reacted with 1-pentene (3 mL, 27.3 mmol) at 55 °C for 2 d. The platinum bromide was filtered off, and the solvent was vacuum-evaporated to give **4** and **5** as white powders.

For **4**: 154.1 mg (0.37 mmol, 68%), mp 32−35 °C. ^{11}B NMR (128.4 MHz, C_6D_6) (int, mult, J_{BH} = Hz) 25.7 (1, s), 23.0 (1, s), 8.5 (1, d, 125), 6.7 (1, s), 6.6 (1, d, ∼160), −0.47 (1, d, ∼173), −2.3 (1, d, ∼157), −6.9 (1, d, ∼129), −36.8 (1, d, 132), −37.5 (1, d, ∼136) ppm. DFT/GIAO-calculated ^{11}B NMR shifts (assign) 23.5 (B9), 18.9 (B6), 10.3 (B3), 9.5 (B5), 5.7 (B1), −0.4 (B10), −5.7 (B8), −9.9 (B7), −39.5 (B2), −40.6 (B4) ppm. $^1H\{^{11}B\}$ NMR (400.1 MHz, C_6D_6) (int, assign) 4.14 (1, BH), 3.85 (1, BH), 3.31 (1, BH), 2.96 (1, BH), 2.82 (1, BH), 1.54 (16, $8CH_2$), 1.16 (6, $2CH_3$), 0.77 (1, BH, br), −1.17 (1, BH, br), −1.64 (BH, br), −1.87 (1, BH, br) ppm (the remaining BH resonances were not resolvable). NCI HRMS: *m/z* calc for $C_{11}H_{33}B_{10}O_3F_3S$: 412.3033, found: 412.3002. IR (NaCl, cm^{-1}): 3210 (m), 2959 (s), 2929 (s), 2873 (m), 2861 (m), 2755 (s), 1924 (w), 1629 (w), 1466 (m), 1399 (s), 1247 (m), 1216 (s), 1147 (s), 1102 (m), 1072 (s), 974 (m), 916 (m), 850 (w), 720 (w), 626 (m), 508 (w).

For **5**: 76.6 mg (0.29 mmol, 76%). ^{11}B NMR (128.4 MHz, D_2O) (int, mult, J_{BH} = Hz) 24.6 (2, s), 10.9 (1, d, 186), 9.3 (1, d, 169), 1.2 (1, d, 144), −2.6 (1, d, 169), −4.2 (1, d, 173), −16.0 (1, d, 39), −34.7 (1, d, 163), −36.0 (1, d, 161) ppm. $^1H\{^{11}B\}$ NMR (400.1 MHz, CD_2Cl_2) (int, assign)

3.88 (1, BH), 3.25 (2, BH), 3.10 (1, BH), 2.92 (1, BH), 1.58 (8, 4CH$_2$), 1.38 (8, 4CH$_2$), 1.06 (1, BH), 0.92 (6, 2CH$_3$), 0.72 (1, BH), −0.03 (1, BH, br), −0.97 (1, BH, br), −1.21 (1, BH, br), −1.34 (1, BH, br) ppm (the remaining BH resonances were not resolvable). IR (NaCl, cm^{-1}): 2956 (s), 2925 (s), 2870 (m), 2552 (w), 1460 (m), 1377 (w), 1260 (m), 1088 (m), 800 (m). Crystals of **5** suitable for a crystallographic determination were obtained by the slow evaporation of a hexanes solution.

5-TfO-6,9-(Me$_2$S)$_2$-B$_{10}$H$_{11}$ (6). After a solution of **1** (500 mg, 1.8 mmol) and dimethylsulfide (3 mL, 4.1 mmol) in toluene (10 mL) was stirred at room temperature for 3 h, a white precipitate formed. The precipitate was collected via filtration, washed with toluene, and dried in vacuo to give pure **6**.

For **6**: 508 mg (1.3 mmol, 70%), mp 69−72 °C. ^{11}B NMR (128.4 MHz, CDCl$_3$) (int, mult, J_{BH} = Hz) −6.0 (1, d, ∼122), −6.3 (1, s), −9.6 (1, d, 132), −22.9 (2, d, ∼149), −24.8 (1, d, br), −26.1 (1, d, ∼175), −27.7 (1, d, ∼179), −40.6 (1, d, 147), −44.9 (1, d, 143) ppm. DFT/GIAO-calculated ^{11}B NMR shifts (assign) −2.8 (B2), −5.3 (B4), −5.8 (B5), −22.0 (B10), −22.3 (B7), −23.4 (B8), −23.8 (B9), −25.0 (B6), −38.4 (B1), −44.8 (B3). ^{1}H{^{11}B} NMR (400.1 MHz, C$_6$D$_6$) (int, assign) 3.25 (2, BH), 2.55 (1, BH), 2.44 (1, BH), 2.13 (2, BH), 1.79 (3, CH$_3$), 1.66 (3, CH$_3$), 1.65 (1, BH), 1.56 (3, CH$_3$), 1.55 (3, CH$_3$), 1.32 (1, BH), −0.14 (2, BH), −1.42 (1, BH) ppm. NCI HRMS: *m/z* calc for C$_5$H$_{24}$B$_{10}$O$_3$F$_3$S$_3$: 395.1770, found: 395.1772. Anal. Calcd: C: 15.26, H: 6.15; found: C: 15.72, H: 5.81%. IR (NaCl, cm^{-1}): 3198 (w), 3022 (w), 2930 (w), 2536 (s), 1428 (m), 1382 (s), 1246 (m), 1206 (s), 1153 (s), 1073 (m), 1035 (m), 988 (s), 960 (s), 921 (m), 637 (m), 625 (m), 510 (m). Crystals of **6** suitable for a crystallographic determination were obtained by the slow evaporation of a hexanes/dichloromethane solution.

Reaction of 6-TfO-B$_{10}$H$_{13}$ with Dimethylsulfide. The reaction of 6-TfO-B$_{10}$H$_{13}$[4] (80 mg, 0.30 mmol) and 2.7 mL (3.0 mmol) of dimethylsulfide in toluene (5 mL) at room temperature for 24 h gave 6,9-(Me$_2$S)$_2$-B$_{10}$H$_{12}$ (20 mg, 0.08 mmol, 27%) along with ∼10% unreacted 6-TfO-B$_{10}$H$_{13}$. The ^{11}B spectrum of 6,9-(Me$_2$S)$_2$-B$_{10}$H$_{12}$ was consistent with that previously reported.[12]

General Procedure for the Syntheses of 1-R-4-TfO-1,2-C$_2$B$_{10}$H$_{10}$ (7−12). A 100 mL Schlenk flask equipped with a stir bar was charged under N$_2$ with **6**, alkyne, and toluene. The flask was sealed and then submerged in an oil bath heated at 70 °C. The stirred reaction was monitored by ^{11}B NMR until all of the **6** was consumed (12−18 h). The solvent and unreacted alkyne were vacuum-evaporated, and the resulting residue was extracted with pentane until all product was removed. The extracts were combined, and the solvent was vacuum-evaporated. All products were purified by silica-gel chromatography using a 50/50 hexanes/CH$_2$Cl$_2$ eluent.

1-C$_6$H$_5$-4-TfO-1,2-C$_2$B$_{10}$H$_{10}$ (7). **6** (200 mg, 0.51 mmol), phenylacetylene (3 equiv 0.17 mL, 1.53 mmol), and toluene (10 mL).

For **7**: colorless oil, 107.6 mg (0.29 mmol, 57%). ^{11}B NMR (128.4 MHz, CD$_2$Cl$_2$) (int, mult, J_{BH} = Hz) −0.6 (1, s), −3.6 (1, d, 155), −5.6 (1, d, 151), −11.1 (2, d, ∼193), −12.6 (3, d, ∼160), −16.4 (1, d, ∼177), −18.2 (1, d, br) ppm. DFT/GIAO-calculated ^{11}B NMR shifts (assign) −1.1 (B4), −2.0 (B7), −5.2 (B12), −10.8 (B8), −11.7 (B5), −12.5 (B11), −15.2 (B6), −17.2 (B9), −17.3 (B3), −19.3 (B10) ppm. ^{1}H{^{11}B} NMR (400.1 MHz, CD$_2$Cl$_2$) (int, assign) 7.4−7.5 (5, C$_6$H$_5$), 3.99 (1, cage-CH), 3.10 (1, BH), 2.86 (1, BH), 2.67 (2, BH), 2.58 (1, BH), 2.40 (1, BH), 2.27 (2, BH), 2.22 (1, BH) ppm. NCI HRMS: *m/z* calc for C$_9$H$_{15}$B$_{10}$O$_3$F$_3$S: 370.1625, found: 370.1631. IR (NaCl, cm^{-1}): 3290 (m), 3027 (m), 2557 (s), 1603 (w), 1495 (m), 1445 (m), 1413 (m), 1213 (s), 1151 (m), 1030 (w), 997 (w), 937 (w), 815 (w), 758 (m), 731 (m), 693 (m), 618 (w).

1-CF$_3$C$_6$H$_4$-4-TfO-1,2-C$_2$B$_{10}$H$_{10}$ (8). **6** (200 mg, 0.51 mmol), trifluoromethylphenylacetylene (3 equiv, 0.23 mL, 1.53 mmol), and toluene (10 mL).

For **8**: colorless oil, 118.4 mg (0.27 mmol, 53%). ^{11}B NMR (128.4 MHz, CD$_2$Cl$_2$) (int, mult, J_{BH} = Hz) 0.9 (1, s), −1.7 (1, d, ∼176), −3.6 (1, d, br), −9.0 (1, d, ∼124), −11.0 (2, d, ∼139), −11.9 (2, d, ∼116), −15.0 (1, d, ∼173), −17.0 (1, d, ∼175) ppm. DFT/GIAO-calculated ^{11}B NMR shifts (assign) −0.9 (B4), −1.8 (B7), −4.2 (B12), −11.0 (B8), −11.6 (B5), −12.6 (B11), −16.0 (B6), −17.0 (B3), −17.4 (B9), −19.5

(B10) ppm. ^{1}H{^{11}B} NMR (400.1 MHz, CD$_2$Cl$_2$) (int, assign) 7.6−7.7 (4, C$_6$H$_4$), 4.15 (1, cage-CH), 3.08 (1, BH), 2.86 (1, BH), 2.80 (1, BH), 2.64 (1, BH), 2.55 (1, BH), 2.40 (1, BH), 2.27 (2, BH) ppm (the remaining BH resonance was not resolvable). NCI HRMS: *m/z* calc for C$_{10}$H$_{14}$B$_{10}$O$_3$F$_6$S: 438.1498, found: 438.1496. IR (NaCl, cm^{-1}): 3073 (m), 2597 (s), 1617 (m), 1411 (s), 1390 (s), 1219 (s), 1171 (s), 1135 (s), 1068 (s), 1020 (m), 989 (m), 924 (m), 848 (m), 616 (m). Crystals of **8** suitable for a crystallographic determination were obtained from slow evaporation of a pentane solution at −20 °C.

1-C$_6$H$_{11}$-4-TfO-1,2-C$_2$B$_{10}$H$_{10}$ (9). **6** (200 mg, 0.51 mmol), cyclohexylacetylene (3 equiv, 0.20 mL, 1.53 mmol), and toluene (10 mL).

For **9**: colorless oil, 120.9 mg (0.32 mmol, 63%). ^{11}B NMR (128.4 MHz, CD$_2$Cl$_2$) (int, mult, J_{BH} = Hz) −0.7 (1, s), −4.5 (1, d, ∼175), −5.9 (1, d, ∼156), −11.0 (1, d, ∼164), −12.5 (3, d, 172), −16.4 (2, d, 173), −19.1 (1, d, ∼147) ppm. DFT/GIAO-calculated ^{11}B NMR shifts (assign) −2.1 (B4), −3.6 (B7), −6.2 (B12), −10.9 (B8), −12.7 (B5), −14.7 (B3), −15.8 (B6), −17.6 (B9), −19.0 (B10) ppm. ^{1}H NMR (400.1 MHz, CD$_2$Cl$_2$) (int, assign) 3.79 (1, cage-CH), 2.36−0.88 (11, C$_6$H$_{11}$) ppm. NCI HRMS: *m/z* calc for C$_9$H$_{21}$B$_{10}$O$_3$F$_3$S: 376.2094, found: 376.2131. IR (NaCl, cm^{-1}): 2926 (s), 2853 (s), 2559 (s), 1449 (w), 1383 (m), 1247 (m), 1207 (s), 1153 (s), 1083 (w), 1040 (w), 1000 (w), 619 (w).

1-CH$_3$(CH$_2$)$_5$-4-TfO-1,2-C$_2$B$_{10}$H$_{10}$ (10). **6** (200 mg, 0.51 mmol), 1-octyne (3 equiv, 0.23 mL, 1.53 mmol), and toluene (10 mL).

For **10**: colorless oil, 94.7 mg (0.26 mmol, 51%). ^{11}B NMR (128.4 MHz, CD$_2$Cl$_2$) (int, mult, J_{BH} = Hz) −1.0 (1, s), −4.0 (1, d, 159), −7.0 (1, d, 149), −12.5 (4, d, br), −14.8 (1, d, ∼140), −16.1 (1, d, ∼171), −19.1 (1, d, ∼186) ppm. ^{1}H NMR (400.1 MHz, CD$_2$Cl$_2$) (int, assign) 3.80 (1, cage-CH), 1.31 (10, 5CH$_2$), 0.89 (3, CH$_3$) ppm. NCI HRMS: *m/z* calc for C$_8$H$_{21}$B$_{10}$F$_3$O$_3$S: 364.2094, found: 364.2098. IR (NaCl, cm^{-1}): 3301 (s), 3025 (m), 2930 (s), 2861 (m), 2557 (s), 2116 (w), 1634 (m), 1383 (m), 1211 (m), 1153 (m), 1030 (m), 998 (m), 735 (m), 697 (w), 638 (m).

1-CH$_3$COOCH$_2$-4-TfO-1,2-C$_2$B$_{10}$H$_{10}$ (11). **6** (200 mg, 0.51 mmol), propargyl acetate (3 equiv, 0.15 mL, 1.53 mmol), and toluene (10 mL).

For **11**: colorless oil, 98.9 mg (0.27 mmol, 53%). ^{11}B NMR (128.4 MHz, CD$_2$Cl$_2$) (int, mult, J_{BH} = Hz) −0.8 (1, s), −3.1 (1, d, 156), −5.3 (1, d, 156), −12.0 (3, d, ∼131), −13.7 (2, d, ∼123), −15.5 (1, d, ∼128), −18.7 (1, d, 139) ppm. DFT/GIAO-calculated ^{11}B NMR shifts (assign) −1.9 (B4), −4.8 (B8), −5.1 (B12), −9.9 (B7), −11.9 (B9), −14.2 (B3), −14.7 (B5), −17.4 (B11), −18.3 (B6), −20.2 (B10) ppm. ^{1}H{^{11}B} NMR (400.1 MHz, CD$_2$Cl$_2$) (int, assign) 4.76 (2, CH$_2$, m), 4.05 (1, cage-CH), 2.70 (1, BH), 2.60 (1, BH), 2.49 (1, BH), 2.38 (2, BH), 2.32 (1, BH), 2.16 (3, CH$_3$) ppm (the remaining BH resonances were not resolvable). NCI HRMS: *m/z* calc for C$_6$H$_{15}$B$_{10}$O$_5$F$_3$S: 366.1523, found: 366.1597. IR (NaCl, cm^{-1}): 3067 (w), 2599 (m), 1758 (m), 1410 (m), 1367 (w), 1290 (s), 1148 (m), 1110 (w), 1054 (w), 1000 (w), 926 (w), 858 (w), 616 (w).

1-BrCH$_2$CH$_2$-4-TfO-1,2-C$_2$B$_{10}$H$_{10}$ (12). **6** (200 mg, 0.51 mmol), 4-bromo-1-butyne (3 equiv, 0.14 mL, 1.53 mmol), and toluene (10 mL).

For **12**: colorless oil, 106.1 mg (0.27 mmol, 52%). ^{11}B NMR (128.4 MHz, CD$_2$Cl$_2$) (int, mult, J_{BH} = Hz) −1.0 (1, s), −3.3 (1, d, 155), −5.8 (1, d, 145), −11.4 (1, d, ∼135), −12.1 (2, d, ∼118), −12.9 (1, d, ∼152), −14.7 (1, d, ∼163), −15.5 (1, d, ∼164), −18.7 (1, d, 164) ppm. ^{1}H{^{11}B} NMR (400.1 MHz, CDCl$_3$) (int, assign) 4.01 (1, cage-CH), 3.05 (2, CH$_2$), 2.90 (2, CH$_2$), 2.72 (1, BH), 2.63 (1, BH), 2.53 (1, BH), 2.45 (1, BH), 2.33 (1, BH), 2.28 (1, BH), 2.15 (2, BH) ppm (the remaining BH resonance was not resolvable). NCI HRMS: *m/z* calc for C$_5$H$_{14}$B$_{10}$O$_3$F$_3$SBr: 400.0730, found: 400.0759. Anal. Calcd: C: 17.51, H: 4.10; found: C: 17.89, H: 4.67%. IR (NaCl, cm^{-1}): 3064 (w), 2928 (m), 2591 (s), 2259 (w), 1635 (w), 1407 (s), 1216 (s), 1150 (s), 1001 (m), 924 (m), 857 (w), 731 (w), 615 (m).

Reaction of 1 with 3-hexyne in bmimCl/Toluene. Following reported procedure,[13] a mixture of **1** (150 mg, 0.56 mmol) and 300 mg (3.7 mmol) of 3-hexyne in a biphasic toluene (5 mL)/bmimCl (100 mg, 0.57 mmol) was reacted at 120 °C for ∼7 min. The toluene layer was removed and vacuum-evaporated to give 1,2-Et$_2$-1,2-C$_2$B$_{10}$H$_{10}$ (72.8 mg, 0.35 mmol, 65%). The ^{11}B and ^{1}H NMR spectra were consistent with those previously reported.[13] NCI HRMS: *m/z* calc C$_6$B$_{10}$H$_{20}$: 202.2802; found: 202.2819.

1- and 2-TfO-$B_{10}H_9{}^{2-}$ (16−19). In separate reactions, a 100 mL Schlenk flask equipped with a stir bar was charged under N_2 with **6** (200 mg, 0.51 mmol). For one reaction, dichloromethane (5 mL) and excess triethylamine (0.1 mL, 0.72 mmol) were added, and the solution was stirred overnight. For the other reaction, excess liquid ammonia (~1 mL, condensed in at 77 K) was added, and then the stirred mixture was allowed to very slowly warm to room temperature while the flask was connected to a pressure-release bubbler. At the conclusion of the reactions, vacuum-evaporation of the solvents and/or excess amines gave a mixture of the ammonium salts of the 1-TfO-$B_{10}H_9{}^{2-}$ and 2-TfO-$B_{10}H_9{}^{2-}$ anions. The [1-TfO-$B_{10}H_9{}^{2-}$] isomers were then selectively precipitated from dichloromethane solutions at −78 °C.

For [Et_3NH^+]$_2$[1-TfO-$B_{10}H_9{}^{2-}$] (16). 72.2 mg (0.15 mmol, 30%). ^{11}B NMR (128.4 MHz, D_2O) (int, mult, J_{BH} = Hz) 19.7 (1, s), −7.8 (1, d, 138), −32.7 (8, d, ~130) ppm. DFT/GIAO-calculated ^{11}B NMR shifts (assign) 20.8 (B1), −6.6 (B10), −29.1 (B5), −29.5 (B3), −29.9 (B4), −30.4 (B2), −33.0 (B9), −33.4 (B7), −35.0 (B6), −35.8 (B8) ppm. DFT/GIAO-calculated shifts assuming TfO rotation: 20.8 (B1), −6.6 (B10), −29.7 (B2,3,4,5), −34.3 (B6,7,8,9) ppm. ^{1}H{^{11}B} NMR (400.1 MHz, D_2O) (int, assign) 4.95 (2, NH), 3.16 (12, 6CH_2), 1.34 (18, 6CH_3) ppm. Anal. Calcd: C: 33.18, H: 8.78, N: 5.95; found: C: 31.22, H: 8.50, N: 5.49%.

For [Et_3NH^+]$_2$[2-TfO-$B_{10}H_9{}^{2-}$] (17). 154.0 mg (0.33 mmol, 64%). ^{11}B NMR (128.4 MHz, CD_3CN) (int, mult, J_{BH} = Hz) −1.1 (1, s), −2.2 (1, d, 140), −5.2 (1, d, 149), −23.5 (1, d, ~167), −24.8 (1, d, ~169), −28.7 (2, d, ~140), −31.4 (3, d, ~105) ppm. DFT/GIAO-calculated ^{11}B NMR shifts (assign) 1.5 (B2), −0.5 (B10), −10.6 (B1), −25.0 (B7/B8), −26.2 (B5), −28.2 (B3), −31.8 (B6), −31.9 (B9), −34.1 (B4) ppm. ^{1}H{^{11}B} NMR (400.1 MHz, D_2O) (int, assign) 5.39 (2, NH), 3.11 (12, 6CH_2), 1.20 (18, 6CH_3) ppm. ESI HRMS: *m/z* calc for $H_9C_1B_{10}F_3SO_3$: 266.1229, found: 266.0788. Anal. Calcd: C: 33.18, H: 8.78, N: 5.95; found: C: 31.73, H: 8.56, N: 5.56%.

For [NH_4^+]$_2$[1-TfO-$B_{10}H_9{}^{2-}$] (18). 60 mg (0.20 mmol, 40%). The ^{11}B NMR spectrum was identical to that observed for **16**. ^{1}H NMR (400.1 MHz, D_2O) (int, assign) 7.1 (8, 2NH_4^+) ppm. ESI LRMS: *m/z* calc for $H_9B_{10}O_3SCF_3$: 268.1155, found: 268.1163.

For [NH_4^+]$_2$[2-TfO-$B_{10}H_9{}^{2-}$] (19). 79 mg (0.26 mmol, 52%). The ^{11}B NMR spectrum was identical to that observed for **17**. ^{1}H{^{11}B} NMR (400.1 MHz, D_2O) (int, assign) 7.1 (8, 2NH_4^+) ppm.

Collection and Reduction of the Data. Crystallographic data and structure refinement information are summarized in Supporting Information, Table S1. X-ray intensity data for **1** (Penn3379), **5** (Penn3396), **6** (Penn3411), **8** (Penn3432), and **18** (Penn3403) were collected on a Bruker APEXII CCD area detector. Preliminary indexing was performed from a series of 36 rotation frames (0.5°) with exposures of 10 s. Rotation frames were integrated using SAINT,[14] producing a listing of unaveraged F^2 and $\sigma(F^2)$ values that were then passed to the SHELXTL program package[15] for further processing and structure solution. All reflections were used during refinement. Non-hydrogen atoms were refined anisotropically; cage hydrogen atoms were refined isotropically, and all other hydrogen atoms were refined using a riding model.

Computational Methods. DFT calculations were performed using the Gaussian 09 package.[16] Unless specifically stated, all ground state, transition state, and intermediate geometries, as well as their electronic and free energies, were obtained using the B3LYP/6-311G(d) level without constraints for all H, C, B, O, F, and S atoms. The B3LYP/SDD pseudopotential was used for the I atom in **6**. The ^{11}B NMR chemical shifts were calculated at the B3LYP/6-311G(d) level using the GIAO option within Gaussian and are referenced to $BF_3·O(C_2H_5)_2$ using an absolute shielding constant of 102.24 ppm. Harmonic vibrational analyses were carried out on the optimized geometries at the same level to establish the nature of stationary points. Transition states were located using the QST2 option in Gaussian 09 and were verified to contain only one imaginary frequency. Continuity of the reaction pathway was confirmed by intrinsic reaction coordinate (IRC) calculations and/or visualization of the imaginary frequencies. All optimized Cartesian coordinates are given in the Supporting Information in Tables S2−S19. Calculated relative electronic energies for selected structures are given in Supporting Information, Table S20.

RESULTS AND DISCUSSION

In contrast to the finding[4] that 6-TfO-$B_{10}H_{13}$ was formed by the room-temperature reaction of *closo*-$B_{10}H_{10}{}^{2-}$ with triflic acid in cyclopentane (eq 2), we observed that the 60 °C reaction of [NH_4^+]$_2$[*closo*-$B_{10}H_{10}{}^{2-}$] with a large excess of triflic acid in the ionic liquid bmimOTf gave exclusively the previously unknown 5-TfO-$B_{10}H_{13}$ (**1**) (eq 4). In a typical reaction, vigorous stirring
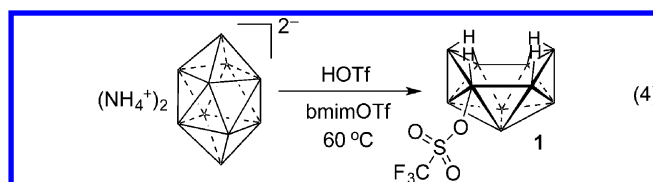
of [NH_4^+]$_2$[*closo*-$B_{10}H_{10}{}^{2-}$] in bmimOTf at 60 °C for 12 h, followed by extraction with hexanes and subsequent recrystallization from pentane, gave crystalline **1** in 64% yield.

The ^{11}B NMR spectra of **1** (Figure 1) were consistent with a C_1 cage-symmetry, displaying eight separate doublet resonances,
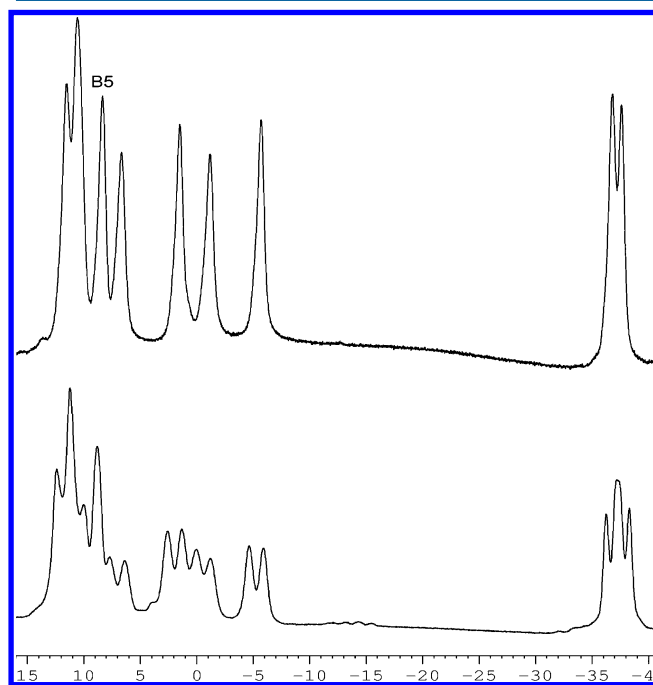

Figure 1. ^{11}B{^{1}H} (top) and ^{11}B (bottom) NMR spectra of **1**.

with the doublet at 11.6 ppm having intensity-two, and one singlet at 9.3 ppm arising from the TfO-substituted boron. The agreement of the observed spectra with the chemical shifts predicted by DFT/GIAO calculations (B3LYP/6-311G(d)) for 5-TfO-$B_{10}H_{13}$ allowed the assignment of the resonances indicated in the Experimental Section. The ^{1}H NMR spectrum of **1** (Figure S1, Supporting Information) was again indicative of C_1 symmetry, with four separate bridging-hydrogen resonances in the same 1-downfield/3-upfield pattern (1 at 0.4 ppm and 3 above 0.0 ppm) previously observed in the spectra of the 5-X-$B_{10}H_{13}$ halogenated derivatives.[6,7] As shown in Figure 2, a single-crystal X-ray diffraction study confirmed the 5-TfO-$B_{10}H_{13}$ structure of **1**.

The B5−O1 distance (1.447(4) Å) in **1** is slightly longer than that found in 6-TfO-$B_{10}H_{13}$ (1.433(4) Å)[4] but is significantly longer than those found in 5-RO-$B_{10}H_{13}$ (R = Me (1.370(3) Å),
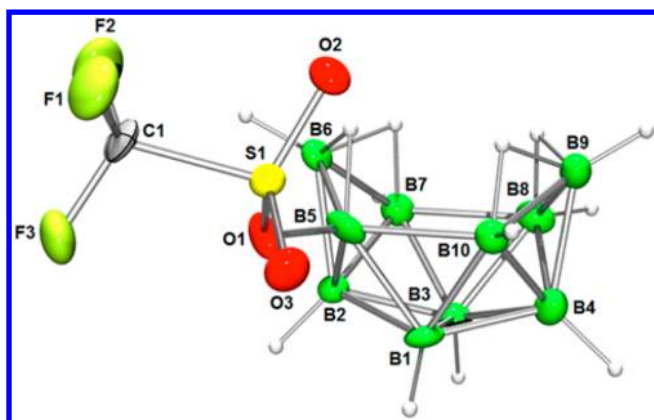
Figure 2. Crystallographically determined structure of **1**. Selected distances (Å) and angles (deg): B5−O1, 1.447(4); B5−B6, 1.797(5); B6−B7, 1.790(5); B7−B8, 1.982(5); B8−B9, 1.778(5); B9−B10, 1.784(5); B5−B10, 1.970(4); B2−B6, 1.730(4); B4−B9, 1.744(5); B4−B10, 1.787(4); B3−B8, 1.752(4); B1−B5, 1.750(4); B2−B5, 1.784(5); B2−B7, 1.796(5); O1−S1, 1.538(2); O2−S1, 1.425(2); O3−S1, 1.417(2); B5−O1−S1, 125.44(19); O1−B5−B6, 119.1(2); O1−B5−B10, 118.1(2); B2−B6−B5, 60.75(18); B7−B6−B5, 101.1(2); B8−B9−B10, 104.9(2); B6−B5−B10, 118.2(2); B6−B7−B8, 117.0(2).

$ClC_2H_4OC_2H_4$ (1.3604(19) Å), and $CH_3C\equiv CCH_2$ (1.3828(17) Å)).[11] These differences are consistent with less O1 → B5 π-bonding in **1**, as is expected for the strongly electron-withdrawing triflate group.

Investigations into the reason for the formation of the different isomers observed in the cyclopentane (eq 1) and bmimOTf (eq 4) reactions revealed that 6-TfO-$B_{10}H_{13}$ readily isomerized to its 5-TfO-$B_{10}H_{13}$ isomer when heated above room temperature in either bmimOTf or toluene solvents (eq 5). For example, when a

(5)

pure sample of 6-TfO-$B_{10}H_{13}$ (prepared as described previously[4]) was heated at 55 °C in bmimOTf in either the presence or absence of added triflic acid, isomerization to **1** was observed within 36 h, providing 78 and 68% isolated yields, respectively. While 6-TfO-$B_{10}H_{13}$ proved to be unreactive in toluene at 55 °C, at 85 °C complete reaction was observed by ^{11}B NMR in 36 h to give a 92% isolated yield of **1** following workup. These observations are consistent with DFT calculations using a variety of basis sets that showed the isomerization of 6-TfO-$B_{10}H_{13}$ to 5-TfO-$B_{10}H_{13}$ to be thermodynamically favorable (B3LYP/6-311G(d), −0.8 kcal/mol; B3LYP/6-311G(d,p), −3.3 kcal/mol; B3LYP/6-311+G(3df,2p), −3.4 kcal/mol, see Supporting Information, Table S20). Thus, both the experimental and computational studies suggest that, as in the cyclopentane reactions, the 6-TfO-$B_{10}H_{13}$ isomer is the likely initial product in the bmimTfO reactions, but because of the higher temperature, efficient isomerization to the energetically favored 5-TfO-$B_{10}H_{13}$ isomer readily occurs.

As shown in Figure 3, DFT (B3LYP/6-311G(d)) analysis identified a unique pathway for the conversion of 6-TfO-$B_{10}H_{13}$ to

Figure 3. DFT-calculated relative electronic energies (kcal/mol) for the thermal isomerization pathway of **6-TfO** to **5-TfO**.

5-TfO-$B_{10}H_{13}$. In the DFT-optimized geometry of 6-TfO-$B_{10}H_{13}$ (**6-TfO** in Figure 3 and Supporting Information, Figure S2), the triflate is bound at its O1 oxygen to B6, but the group has sufficient range of motion that one of its other oxygens can interact with B5. In **TS1**, the incoming triflate O2 atom approaches B5 (O2···B5, 3.46 Å), pushing the *exo* B5-hydrogen toward an *endo* cage position, with the B6−O1 length increasing slightly from the 1.43 Å in **6-TfO** to 1.45 Å in **TS1**. As O2 continues to approach B5, the system decreases in energy until arriving at **INT1**, which is 24.0 kcal/mol higher than **6-TfO**. As shown in Supporting Information, Figure S2 (bottom), in **INT1** the triflate O1−S−O2 unit (104.9°) spans the B5−B6 edge, forming a five-membered ring, with the increased B6−O1 distance (1.76 Å) now close to the decreased length of B5−O2 (1.77 Å). The former B5 *exo*-hydrogen is *endo* at B5, and the hydrogen originally bridging the B6−B5 edge has moved to the *endo* position on B6. The hydrogen originally bridging the B6−B7 edge is *endo* at B7. In **TS2**, the B5−O2 length has decreased to 1.48 Å as the B6−O1 length increased to 2.37 Å, with **TS2** being only slightly higher in energy than **INT1**. As O1 loses all contact with B6, the B6 *endo*-hydrogen moves to the *exo* position, while the B7 and B5 *endo*-hydrogens move to bridging positions on the B6−B7 and B6−B5 edges. This process, along with a shortening of the B5−O2 bond to 1.44 Å, results in the formation of **5-TfO′**, which is then converted to the **5-TfO** optimized structure of **1** (Supporting Information, Figure S2) through a rotation about the B5−O2 bond, falling −0.8 kcal/mol relative to **6-TfO**. This DFT analysis suggests that the facile 6-TfO- to 5-TfO-$B_{10}H_{13}$ isomerization is aided by the unique ability of the triflate group to adopt a bidentate configuration spanning the B6−B5 edge that facilitates the migration of the TfO group to the B5 position.

While the neutral 6-X-$B_{10}H_{13}$ (X = Cl, Br, I) haloboranes have not been observed to thermally isomerize, they have been shown to convert at room temperature to their 5-X-$B_{10}H_{13}$ isomers in the presence of catalytic amounts of base.[7] It was similarly found that the reaction of 6-TfO-$B_{10}H_{13}$ with 5 mol % triethylamine in toluene solution at room temperature resulted in isomerization to **1** (70% isolated yield) in only ~1 h (eq 6).

(6)
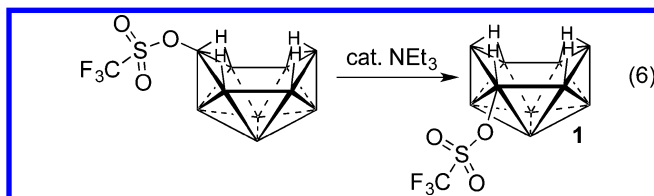
This result is consistent with the previously proposed mechanistic pathway for the base-catalyzed isomerization of the halo-decaboranes involving initial formation of the 6-X-$B_{10}H_{12}^{1-}$ anion, which then isomerizes to 5-X-$B_{10}H_{12}^{1-}$ with subsequent reprotonation to form 5-X-$B_{10}H_{13}$.[7] DFT calculations confirmed that the 5-TfO-$B_{10}H_{12}^{1-}$ anion is of lower energy (−1.35 kcal/mol) than the 6-TfO-$B_{10}H_{12}^{1-}$ anion (Supporting Information, Table S20).

Reactivity Studies of 5-TfO-$B_{10}H_{13}$. The efficient syntheses of **1** described above allowed a systematic investigation of the chemistry of this potentially important starting material. **1** has a number of reactive sites including: (1) Brønsted acidic bridging-hydrogens; (2) a triflate group that could be substituted by metathesis reactions; (3) B6−H and B9−H groups capable of hydroborating olefins; and (4) Lewis acidic borons (B6 and B9) that can coordinate to Lewis bases. Initial examples of these types of reactions are presented in the following sections.

Deprotonation: 5-TfO-$B_{10}H_{12}^{1-}$ (1⁻). When **1** was reacted with 1 equiv of the strong Brønsted base Proton Sponge, deprotonation to form the 5-TfO-$B_{10}H_{12}^{1-}$ (**1⁻**) anion resulted. Depending upon which bridging hydrogen is removed, four different structures are possible for this anion (Supporting Information, Figure S3). DFT calculations indicated the structure in Figure 4, where the hydrogen bridging the B5−B6
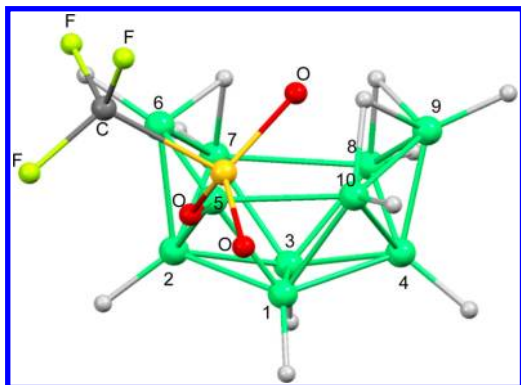
Figure 4. DFT-optimized geometry of **1⁻**.

edge in **1** was removed, to be lowest in energy (Supporting Information, Table S20), and the GIAO-calculated ^{11}B shifts for this structure are in excellent agreement with the experimentally observed spectrum (Figure 5). This structure is likewise consistent with the structure previously confirmed[7] for 5-Cl-$B_{10}H_{12}^{1-}$.
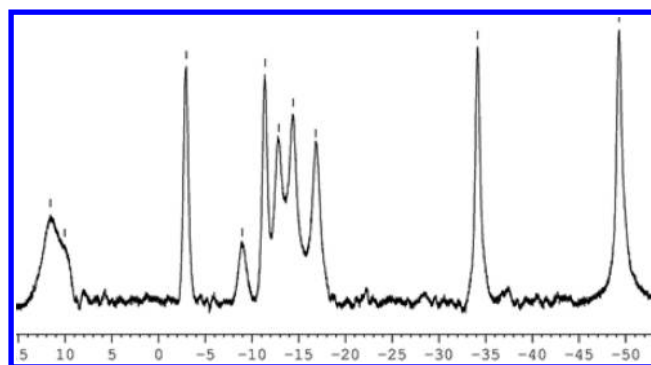
Figure 5. ^{11}B{^{1}H} NMR spectrum of **1⁻**. DFT/GIAO-calculated ^{11}B NMR shifts (assign): 16.4 (B6), 15.4 (B5), 6.3 (B1), −5.8 (B8), −6.6 (B3), −9.3 (B10), −13.6 (B7), −13.9 (B9), −29.8 (B2), −47.5 (B4) ppm.

*TfO-Substitution Reactions: 6-RO-$B_{10}H_{13}$ (R = Me (**2**), 4-CH_3O-C_6H_4O (**3**)).* Nucleophilic attack of alcohols on 5-X-$B_{10}H_{13}$ haloboranes was previously shown to result in halogen substitution by an alkoxide to yield 6-RO-$B_{10}H_{13}$ ethers.[11] Likewise, when **1** was reacted with methanol, clean conversion to 6-MeO-$B_{10}H_{13}$ (**2**) was observed (eq 7) with the 80% isolated

(7)

R = CH_3 **2**
= $C_6H_4OCH_3$ **3**
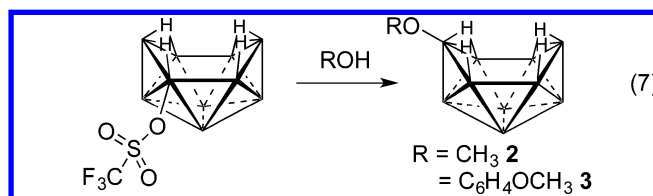
yield of **2** being significantly higher than that from the analogous reaction of methanol with 5-Br-$B_{10}H_{13}$ (54% yield). While the 5-X-$B_{10}H_{13}$ haloboranes had been found to be unreactive toward phenols, **1** readily reacted with *para*-methoxyphenol at 70 °C to give 6-(4-CH_3O-C_6H_4O)-$B_{10}H_{13}$ (**3**) in an 84% isolated yield. The ^{11}B NMR spectra of **3** were similar to those of **2**, with a C_s symmetric pattern (Supporting Information, Figure S4) and with the substituted B6 boron appearing in its predicted downfield position at 22.1 ppm. Again consistent with C_s cage symmetry, the ^{1}H NMR spectrum exhibited two separate intensity-two bridge-hydrogen resonances (Supporting Information, Figure S5).

The formation of the 6-substituted 6-RO-$B_{10}H_{13}$ derivatives starting from 5-TfO-$B_{10}H_{13}$ is consistent with the observed formation of 6-RO-$B_{10}H_{13}$ products in the reaction of alcohols with 5-X-$B_{10}H_{13}$ (X = Cl, Br, I). DFT studies of the MeOH/5-Cl-$B_{10}H_{13}$ reaction[11] indicated that this reaction proceeds by initial nucleophilic attack of the alcohol at B6 to form a transition state in which the B5−B6 bridging hydrogen moves to an *endo* position on B5. Then as HCl is eliminated from B5, the B6 hydrogen moves to the B5−B6 bridging position to produce 6-MeO-$B_{10}H_{13}$. A similar pathway with HOTf elimination at B5 can likewise account for formation of **2** and **3** in the MeOH/5-TfO-$B_{10}H_{13}$ and 4-CH_3O-C_6H_4OH/5-TfO-$B_{10}H_{13}$ reactions.

*Alkene Hydroborations: 5-X-6,9-$(C_5H_{11})_2$-$B_{10}H_{11}$ (X = TfO (**4**), I (**5**)).* Platinum bromide has previously been shown to catalyze olefin hydroborations by both $B_{10}H_{14}$ and its 6-R-$B_{10}H_{12}$ and 6-X-$B_{10}H_{13}$ (X = Cl, I) derivatives to form 6,9-R_2-$B_{10}H_{12}$,[17] 6,9-R,R′-$B_{10}H_{12}$,[18] and 6-X-9-R-$B_{10}H_{12}$[8] alkyl-derivatives, respectively. Likewise, when **1** or its 5-I-$B_{10}H_{13}$ analogue was stirred in neat 1-pentene at 55 °C for 2 d, 5-TfO-6,9-$(C_5H_{11})_2$-$B_{10}H_{11}$ (**4**) and

5-I-6,9-$(C_5H_{11})_2$-$B_{10}H_{11}$ (**5**) were produced in 68 and 76% isolated yields, respectively (eq 8).
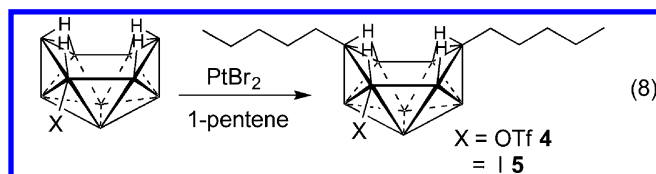
The ^{11}B NMR spectra for both compounds were similar and in excellent agreement with their DFT/GIAO-calculated values, with the triflate-substituted B5 in **4** appearing at 6.7 ppm and the two singlets arising from alkyl-substituted B6 and B9 farther downfield at 25.7 and 23.0 ppm (Supporting Information, Figure S6). In the ^{11}B NMR spectrum of **5**, the alkyl-substituted B6 and B9 resonances again appear downfield as broad overlapped peaks (centered at 24.6 ppm), but the iodinated B5 resonance appears upfield (−16.0 ppm), which is similar to its position in 5-I-$B_{10}H_{13}$ (−13.6 ppm[19]). As can be seen in Figure 6, the B5 resonance in **5**
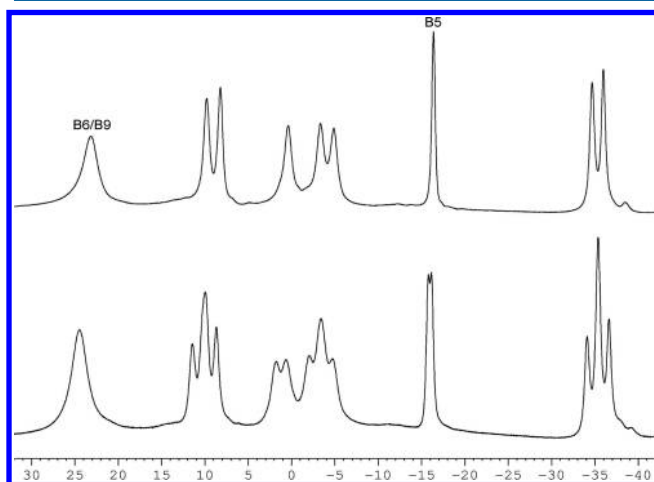
Figure 6. $^{11}B\{^1H\}$ (top) and ^{11}B (bottom) NMR spectra of **5**.

also shows clear doublet fine-structure, with a coupling constant value ($J = 39$ Hz) consistent with the coupling of B5 to the bridging hydrogen at the B5−B6 edge. The $^1H\{^{11}B\}$ NMR spectra of both compounds show four separate bridge-hydrogen resonances (Supporting Information, Figures S7 and S8).

While **4** was isolated as an oil, **5** was obtained as a crystalline solid. A structural determination of **5** (Figure 7) confirmed anti-Markovnikov hydroboration of 1-pentene by the B6−H and B9−H groups, with the observed B6−C1 and B9−C6 distances (both 1.571(3) Å) being similar to those previously reported for 6-alkyldecaboranes.[18,20] Both the B5−I1 (2.180(2) Å) and B5−B6 (1.816(3) Å) distances in **5** are elongated relative to those found[6] in 5-I-$B_{10}H_{13}$ (B5−I, 2.166(5); B5−B6, 1.788(7) Å).

Formation of Lewis Acid−Lewis Base Adducts: 5-TfO-6,9-$(Me_2S)_2$-$B_{10}H_{11}$ (6). Decaborane is known to react with Lewis bases, such as dialkylsulfides or acetonitrile, to form adducts at its Lewis acidic B6 and B9 borons. Such *arachno*-6,9-$L_2B_{10}H_{12}$ compounds are key starting materials for carborane syntheses.[21] However, decaborane derivatives with substitution at one of the B6 or B9 boron positions exhibit lower Lewis acidities than the parent decaborane, and as a result, neither the 6-X-$B_{10}H_{13}$ nor 6-R-$B_{10}H_{13}$ derivatives form adducts at B9 upon reaction with bases. We likewise did not observe B9 adduct formation when 6-TfO-$B_{10}H_{13}$ was reacted with dimethylsulfide. On the other hand, when **1** was reacted with a large excess of dimethylsulfide in toluene at room temperature for 3 h, the diadduct **6** precipitated as a white solid and was isolated in 70% yield (eq 9).
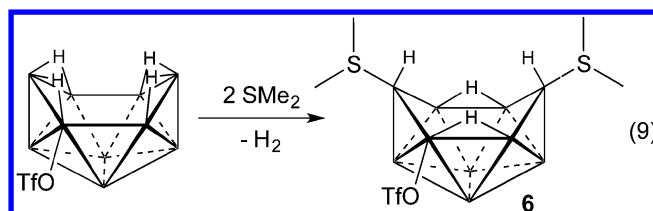
The ^{11}B NMR spectra of **6** (Supporting Information, Figure S9) are consistent with its predicted C_1 symmetry, displaying eight doublets (with the doublet at −22.9 ppm of intensity-two) along with a singlet resonance, at −6.3 ppm, for the triflate-substituted B5 that overlaps the lowest-field doublet. The DFT/GIAO calculations for **6** are again in good agreement with the experimental ^{11}B NMR data. The $^1H\{^{11}B\}$ NMR spectrum of **6** (Supporting Information, Figure S10) also indicated C_1 cage symmetry, with two bridging-hydrogen resonances and four separate methyl resonances.

The single-crystal X-ray determination shown in Figure 8 confirmed **6** to have a cage structure similar to those observed for other *arachno*-6,9-$L_2B_{10}H_{12}$ derivatives,[22] with the two bridging
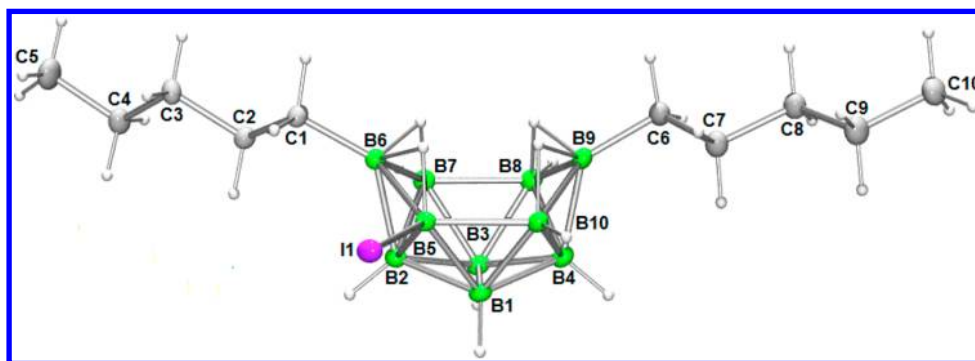

Figure 7. Crystallographically determined structure of **5**. Selected distances (Å) and angles (deg): I1−B5, 2.180(2); B6−C1, 1.571(3); B9−C6, 1.571(3); B5−B6, 1.816(3); B6−B7, 1.800(3); B7−B8, 1.960(4); B8−B9, 1.804(3); B9−B10, 1.800(3); B5−B10, 1.977(3); B4−B9, 1.736(3); B2−B6, 1.736(3); B2−B5, 1.795(3); B2−B7, 1.796(3); B3−B7, 1.755(3); B1−B10, 1.764(3); B1−B5, 1.750(4); B4−B10, 1.790(3); B6−B5−I1, 118.76(14); B2−B5−B6, 57.48(12); B4−B10−B9, 57.83(13); B7−B6−B5, 102.33(15); B10−B9−B8, 103.67(16); C2−C1−B6, 112.59(16); C6−B9−B4, 129.98(19); C1−B6−B2, 130.18(18); B10−B5−I1, 115.70(12).
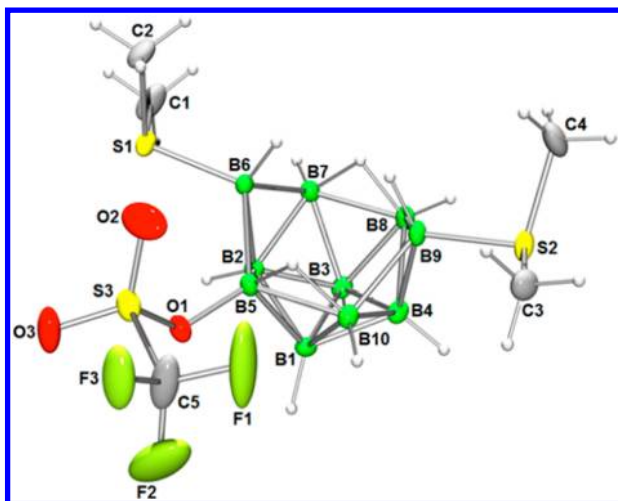
Figure 8. Crystallographically determined structure of **6**. Selected distances (Å) and angles (deg): B5−O1, 1.497(2); B6−S1, 1.9143(19); B9−S2, 1.917(2); B5−B6, 1.829(3); B6−B7, 1.883(3); B7−B8, 1.863(3); B8−B9, 1.866(3); B9−B10, 1.850(3); B5−B10, 1.864(3); B4−B9, 1.743(3); B2−B6, 1.746(3); B1−B4, 1.753(3); B1−B5, 1.767(3); B2−B5, 1.757(3); B3−B7, 1.778(3); S3−O2, 1.412(2); S3−O1, 1.5117(14); S3−O3, 1.4067(18); B5−O1−S3, 127.90(12); O1−B5−B6, 122.96(14); O1−B5−B10, 118.87(15); C2−S1−B6, 102.97(10); C1−S1−B6, 105.43(10); C4−S2−B9, 102.66(10); C3−S2−B9, 104.71(10); B4−B9−S2, 106.40(12); B10−B9−B8, 105.11(13); B5−B6−B7, 103.88(13); B2−B6−S1, 107.95(12).

hydrogens spanning the B5−B10 and B7−B8 edges. In **6**, the O1−B5 distance (1.497(2) Å) is significantly longer and the S3−O1 (1.5117(14) Å) distance is shorter than their corresponding distances in **1** (1.447(4) and 1.538(2) Å, respectively), suggesting less O1 → B5 π-bonding with the more electron-rich **6** *arachno* framework than with the **1** *nido* cage. The biggest effect of the B5-bonded TfO group on the cage framework appears to be on the B5−B6 distance (1.829(3) Å), which is considerably shortened relative to the B6−B7 (1.883(3) Å), B9−B8 (1.866(3) Å), and B9−B10 (1.850(3) Å) distances.

Alkyne Reactions with 5-TfO-6,9-(Me$_2$S)$_2$-B$_{10}$H$_{11}$: Syntheses of Triflate-Functionalized ortho-Carboranes (7−12). Decaborane and its 6,9-(R$_2$S)$_2$-B$_{10}$H$_{12}$ derivatives are key compounds along the synthetic pathway to the C$_2$B$_{10}$ series of carboranes.[21] These carboranes have many technological and/or medical applications,[2] but in many cases their use requires vertex-specific functionalization. While straightforward methods are now available to C-substituted carboranes,[21] selective routes to B-functionalized compounds are less well-developed. One of the most common B-substituted carborane derivatives is the B-halocarboranes, and a number of methods have been developed that allow substitution at different boron sites.[21a] The triflate group is often used as a pseudohalogen in many types of organic palladium-coupling and nucleophilic substitution reactions, and recent studies[23] of C-substituted triflated carboranes also suggest a similar utility for polyborane cluster derivatization. However, B-triflated *ortho*-carboranes have not been available for these applications. The availability of **1** and **6** suggested the possibility of employing these compounds as starting materials for the syntheses of such derivatives.

We recently reported that *ortho*-carboranes can be efficiently synthesized by the reaction of decaborane with alkynes in biphasic ionic liquid/toluene solutions.[13] Analogous biphasic ionic liquid/toluene reactions of 6-R-B$_{10}$H$_{13}$ derivatives with alkynes were also
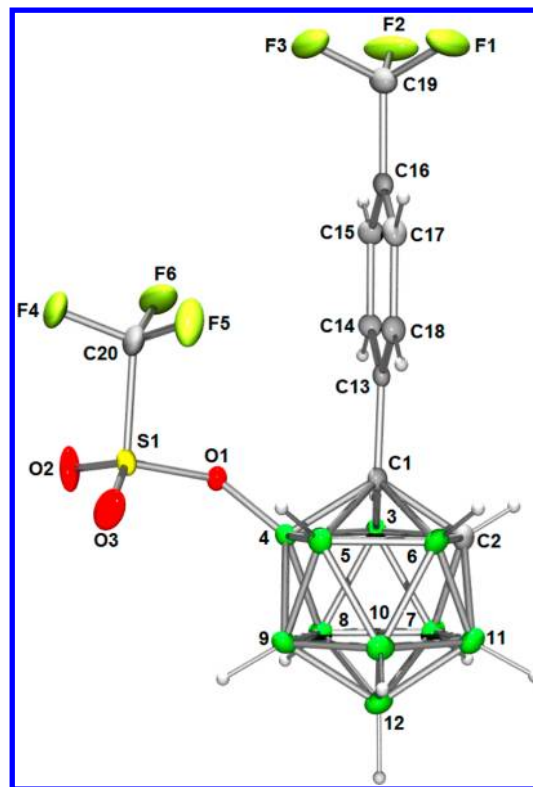

Figure 9. Crystallographically determined structure of **8**. Selected distances (Å) and angles (deg): B4−O1, 1.451(3); C1−C13, 1.506(3); C1−C2, 1.671(4); C1−B6, 1.696(4); C1−B4, 1.722(4); C1−B5, 1.726(4); C1−B3, 1.750(4); C2−B6, 1.702(4); C2−B11, 1.714(4); C2−B7, 1.721(4); C2−B3, 1.729(4); B3−B8, 1.769(4); B3−B7, 1.771(4); B3−B4, 1.782(4); B4−B9, 1.767(4); B4−B8, 1.772(4); B4−B5, 1.777(4); B5−B6, 1.759(4); B5−B10, 1.776(4); B5−B9, 1.781(4); B6−B10, 1.745(4); B6−B11, 1.746(4); B7−B12, 1.774(5); B7−B11, 1.776(5); B7−B8, 1.784(4); B8−B12, 1.783(4); B8−B9, 1.794(4); B9−B10, 1.788(4); B9−B12, 1.791(5); B10−B11, 1.775(5); B10−B12, 1.785(5); B11−B12, 1.768(5); S1−O1, 1.5375(17); S1−O2, 1.407(2); Si−O3, 1.403(2); B4−O1−S1, 130.45(16); C13−C1−C2, 119.9(2); C13−C1−B4, 122.0(2); O1−B4−1, 116.0(2); O1−B4−B3, 114.1(2).

found to give high yields of B-alkyl derivatives[13b,4b] 3- or 4-R-1, 2-C$_2$B$_{10}$H$_{10}$. Unfortunately, this method proved unsuitable for reactions with **1**. While alkyne insertion was achieved, the triflate substituent was not retained with, for example, the reaction of **1** and 3-hexyne, producing only 1,2-Et$_2$C$_2$B$_{10}$H$_{10}$.

The more traditional method for carborane synthesis has employed the reaction of decaborane and an alkyne in the presence of a Lewis base, such as a dialkylsulfide,[21] with the initial step in this reaction proposed to involve the formation of a 6, 9-(R$_2$S)$_2$-B$_{10}$H$_{12}$ complex. Dissociation of one Me$_2$S from this adduct then enables alkyne association to form a 6-(RC≡CH)-9-(Me$_2$S)-B$_{10}$H$_{12}$ intermediate. The loss of the second dimethylsulfide and H$_2$ allows alkyne insertion into the open face of the decaborane cage to form the *ortho*-carborane structure.[24] The report[25] that acetylene insertion into *arachno*-2-Br-6,9-(Et$_2$S)$_2$-B$_{10}$H$_{11}$ produced a mixture of B-bromonated C$_2$B$_{10}$-carboranes suggested that **6** could be employed as a precursor to B-triflated *ortho*-carboranes.

6 was found to react with a variety of terminal alkynes to give the corresponding 1-R-4-TfO-1,2-C$_2$B$_{10}$H$_{10}$ *ortho*-carborane derivatives (eq 10). In these reactions, **6** was stirred with 3 equiv of the corresponding alkyne in toluene at 70 °C until ^{11}B
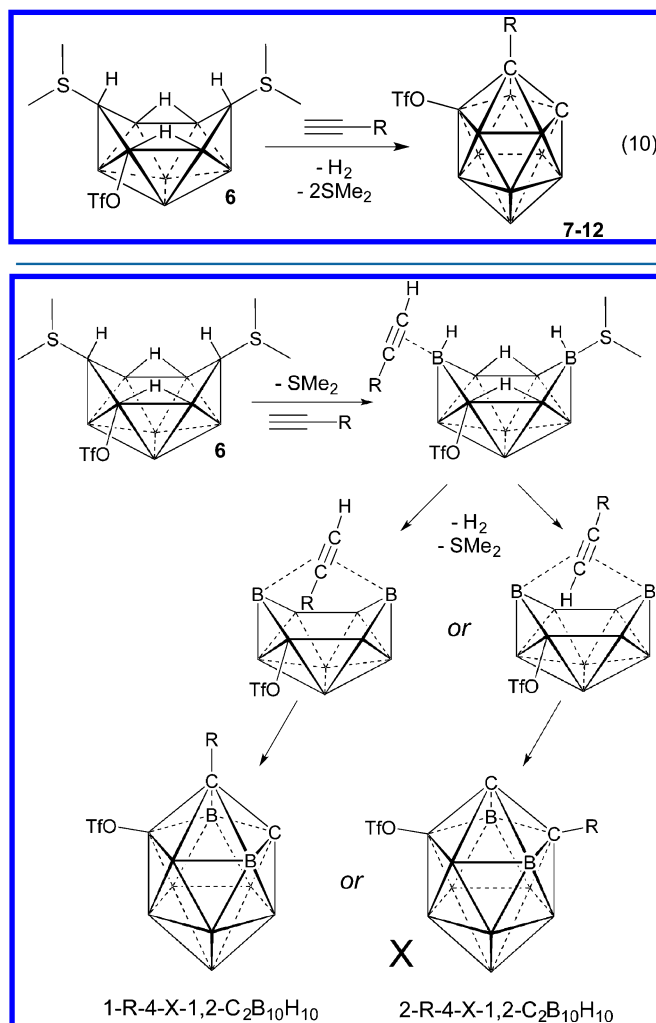
Figure 10. Possible carborane products depending upon alkyne orientation during insertion.

Figure 11. $^{11}B\{^1H\}$ NMR spectrum of (top) 1-TfO-$B_{10}H_9^{2-}$; (bottom) 2-TfO-$B_{10}H_9^{2-}$.

NMR analysis indicated the reaction was complete. After evaporation of the solvent, the remaining oily residues were extracted with hexanes to give the crude *ortho*-carborane products. Purification by silica-gel column chromatography using 50/50 hexanes/CH_2Cl_2 eluent gave the pure carboranes in 51−63% isolated yields. All products were obtained as clear oils at room temperature.

The ^{11}B NMR spectra of all 1-R-4-TfO-1,2-$C_2B_{10}H_{10}$ derivatives were quite similar, with the singlet resonance arising from the TfO-substituted B4 vertex in the 0.9 to −1.0 ppm range. Representative ^{11}B and ^1H NMR spectra are shown in Supporting Information, Figures S11 and S12 for **11**. DFT/GIAO calculations allowed the assignment of the resonances for **7−12** given in the Experimental Section.

As shown in Figure 9, the structure of **8** was confirmed by a single-crystal X-ray diffraction study of crystals grown at −20 °C in pentane (Figure 9). The bond lengths in **8** are nearly identical to those found in a nontriflated carborane with a similar organic substituent (1-(3-HC≡CC$_6$H$_4$)-1,2-$C_2B_{10}H_{11}$).[13a] The B4−O1 distance (1.451(3) Å) of **8** is similar to that observed for **1** (1.447(4) Å).

It is perhaps surprising that only one product was observed in each of the reactions of **6** with a terminal alkyne. On the basis of the previously proposed pathway[24] for alkyne insertion, two different isomers, 1-R-4-X-1,2-$C_2B_{10}H_{10}$ and 2-R-4-X-1,-
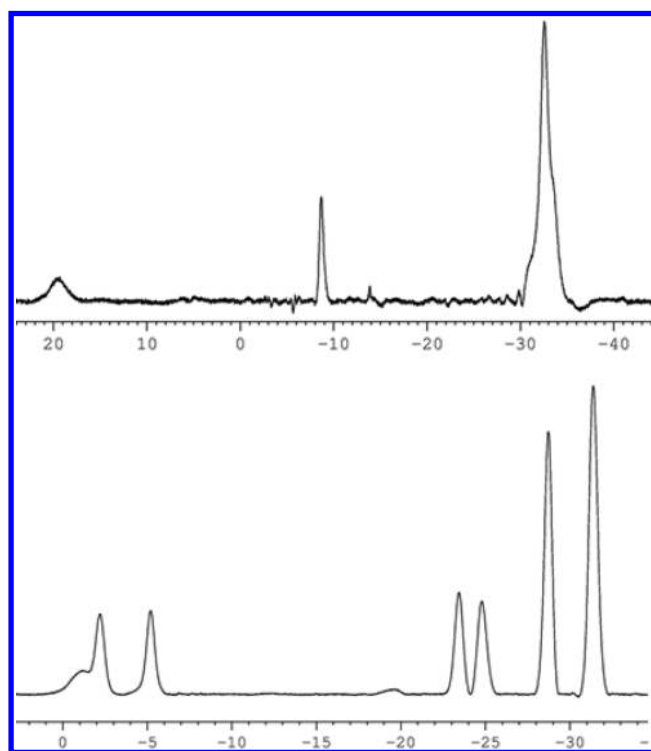
2-$C_2B_{10}H_{10}$, should be possible depending upon the alkyne orientation during insertion (Figure 10). However, in all cases, both the NMR data and TLC analyses of the reactions with **6** indicated only one product was formed. In the 2-R-4-X-1,2-$C_2B_{10}H_{10}$ isomer, the H-substituted carbon is adjacent to the B-OTf, while in the 1-R-4-X-1,2-$C_2B_{10}H_{10}$ isomer the R-substituted carbon is adjacent to the B-OTf. The greater substituent−triflate steric interactions would appear to disfavor the 1-R-4-X-1,2-$C_2B_{10}H_{10}$ isomer where the two groups are adjacent and, indeed, the DFT-calculated energies for the two isomers (Supporting Information, Table S20, R = Me) indicated that the 2-R-4-X-1,2-$C_2B_{10}H_{10}$ isomer is lowest in energy. Nevertheless, the structural determination confirmed that **8** is the 1-R-4-X-1,2-$C_2B_{10}H_{10}$ isomer. This suggests that **7−12** are kinetic products that could possibly result from an initial sterically favorable step where alkyne coordination occurs at its less-hindered CH carbon on the unsubstituted B6−B7−B8−B9 side of the cage before final insertion into the cage framework.

Cage-Closing Reactions of 6: Syntheses of closo-1-TfO-$B_{10}H_9^{2-}$ (16, 18) and closo-2-TfO-$B_{10}H_9^{2-}$ (17, 19) Salts. The previous report[26] that the reactions of 5-X-6,9-(Me$_2$S)$_2$-$B_{10}H_{11}$ with liquid ammonia produce the halo-substituted *closo*-2-X-$B_{10}H_9^{2-}$ anions (X = F, Br, I) suggested that similar reactions with **6** could provide the first route to TfO-substituted decaborates.

The reaction of **6** with excess triethylamine produced a mixture of the [Et$_3$NH$^+$]$_2$[1-TfO-$B_{10}H_9^{2-}$] (**16**) and [Et$_3$NH$^+$]$_2$[2-TfO-$B_{10}H_9^{2-}$] (**17**) isomers in 30 and 64% yields, while the analogous reaction with liquid ammonia gave [NH$_4^+$]$_2$[1-TfO-$B_{10}H_9^{2-}$] (**18**) and [NH$_4^+$]$_2$[2-TfO-$B_{10}H_9^{2-}$] (**19**) in 40 and 52% yields (eq 11).

In both reactions, the two products could be separated by the selective precipitation of the less-soluble **16** and **18** salts. The ^{11}B NMR patterns and chemical shifts for both isomers are in
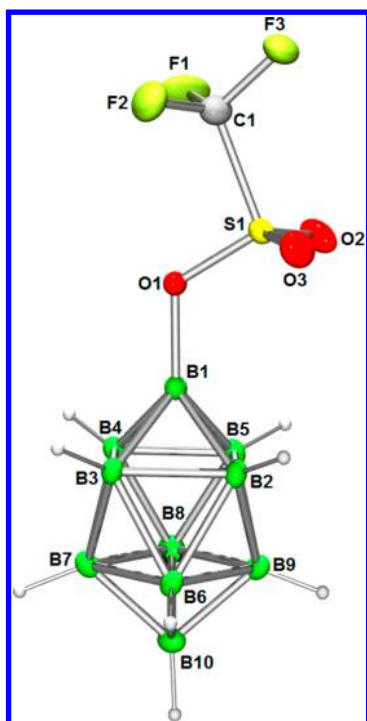
Figure 12. Crystallographically determined structure of **18**. Selected distances (Å) and angles (deg): B1−O1, 1.487(4); B1−B2, 1.677(5); B1−B5, 1.681(5); B1−B4, 1.683(5); B1−B3, 1.683(4); B2−B9, 1.804(5); B2−B6, 1.818(5); B2−B5, 1.840(5); B2−B3, 1.848(5); B3−B6, 1.803(5); B3−B7, 1.805(5); B3−B4, 1.844(4); B4−B8, 1.817(5); B4−B7, 1.823(4); B4−B5, 1.848(5); B5−B8, 1.812(5); B5−B9, 1.813(5); B6−B10, 1.702(5); B6−B7, 1.836(5); B6−B9, 1.837(5); B7−B10, 1.708(5); B7−B8, 1.844(5); B8−B10, 1.702(5); B8−B9, 1.844(5); B9−B10, 1.702(5); S1−O3, 1.4317(2); S1−O2, 1.416(2); S1−O1, 1.505(2); B1−O1−S1, 129.27(19); O1−B1−B2, 132.2(3); O1−B1−B4, 125.6(3); O1−B1−B3, 126.6(3); O1−B1−B5, 131.6(3).

excellent agreement with their DFT/GIAO-calculated values. Consistent with the ^{11}B NMR spectra of 1-HO-$B_{10}H_9^{2-}$[27] and other 1-substituted derivatives,[2] the spectra of **16** and **18** showed
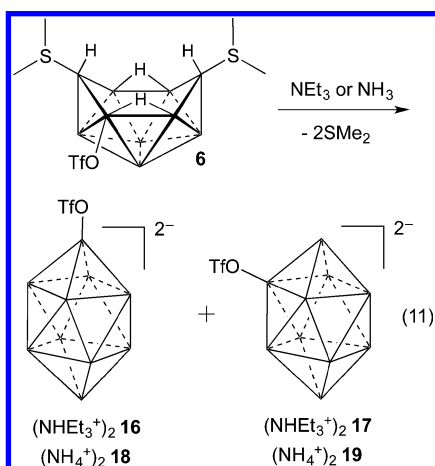
three resonances in 1:1:8 ratios (Figure 11, top), with the singlet resonance for the TfO-substituted B1 appearing at lowest field (19.7), the antipodal B10 resonance at midfield (−7.8 ppm), and the overlapping resonances from the B2,3,4,5 and B6,7,8,9 belts at highest field. Consistent with its DFT/GIAO-calculated values for the C_1 symmetric framework shown in Supporting

Information, Figure S13, the ^{11}B NMR spectrum of the 2-TfO-$B_{10}H_9^{2-}$ anion (**17** and **19**) exhibited seven resonances (with the peak at −28.7 ppm of intensity-two and the −31.4 ppm peak of intensity-three), with the triflate-substituted B2 singlet resonance appearing at −1.1 ppm.

As shown in Figure 12, the structure of $[NH_4^+]_2[1\text{-TfO-}B_{10}H_9^{2-}]$ (**18**) was confirmed by a single-crystal X-ray determination. The B1−O1 bond distance (1.487(3) Å) is longer than that observed for **1** (1.447(4) Å). The cage distances are similar to those in the previously reported[28] structure of $[1\text{-I-}B_{10}H_9^{2-}]$, indicating the substituent has little effect on cage-bonding.

In summary, ionic liquid/triflic acid cage-opening reactions of *closo*-$B_{10}H_{10}^{2-}$ now provide a convenient synthetic route to 5-TfO-$B_{10}H_{13}$. As illustrated by the initial reactivity studies reported herein, this compound and its derivatives should now prove to be valuable new starting materials for the construction of more complex B-substituted polyboranes and carboranes.

■ ASSOCIATED CONTENT

ⓢ Supporting Information

Figures of DFT-optimized geometries, a table of crystallographic data, tables of the coordinates and energies of DFT-optimized structures, ^{11}B and ^1H NMR spectra. This material is available free of charge via the Internet at http://pubs.acs.org.

■ AUTHOR INFORMATION

Corresponding Author

*Email: lsneddon@sas.upenn.edu.

Notes

The authors declare no competing financial interest.

■ ACKNOWLEDGMENTS

■ REFERENCES

(1) (a) Makhlouf, J. M.; Hough, W. V.; Hefferan, G. T. *Inorg. Chem.* **1967**, *6*, 1196−1198. (b) Guillevic, G.; Dazord, J.; Mongeot, H.; Cueilleron, J. *J. Chem. Res., Synop.* **1978**, 402−403. (c) Spalding, T. R.; Power, D. *Polyhedron* **1985**, *4*, 1329−1331. (d) Mongeot, H.; Bonnetot, B.; Atchekzaï, J.; Colombier, M.; Vigot-Vieillard, C. *Bull. Soc. Chim. Fr.* **1986**, 385−389. (e) Colombier, M.; Atchekzaï, J.; Mongeot, H. *Inorg. Chim. Acta* **1986**, *115*, 11−16.

(2) For excellent reviews of the chemistry of the *closo*-$B_{10}H_{10}^{2-}$ anion before 2010 see: (a) Zhizhin, K. Y.; Zhdanov, A. P.; Kuznetsov, N. T. *Russ. J. Inorg. Chem.* **2010**, *55*, 2089−2127. (b) Sivaev, I. B.; Prikaznov, A. N.; Naoufal, D. *Collect. Czech. Chem. Commun.* **2010**, *75*, 1149−1199.

(3) (a) *Boron Science: New Technologies and Applications*; Hosmane, N. S., Ed.; CRC Press: Boca Raton, FL, 2011. (b) Hawthorne, M. F. *Angew. Chem., Int. Ed.* **1993**, *32*, 950−984. (c) Barth, R. F.; Soloway, A. H.; Fairchild, R. G. *Sci. Am.* **1990**, 100−107. (d) Soloway, A. H.; Tjarks, W.; Barnum, B. A.; Rong, F.-G.; Barth, R. F.; Codogni, I. M.; Wilson, J. G. *Chem. Rev.* **1998**, *98*, 1515−1562. (e) Armstrong, A. F.; Valliant, J. F. *Dalton Trans.* **2007**, 4240−4251. (e) Sivaev, I. B.; Bregadze, V. V. *Eur. J. Inorg. Chem.* **2009**, 1433−1450.

(4) (a) Hawthorne, M. F.; Mavunkal, I. J.; Knobler, C. B. *J. Am. Chem. Soc.* **1992**, *114*, 4427−4429. (b) Bondarev, O.; Sevryugina, Y. V.; Jalisatgi, S. S.; Hawthorne, M. F. *Inorg. Chem.* **2012**, *51*, 9935−9942.

(5) Naoufal, D.; Kodeih, M.; Cornu, D.; Miele, P. J. *J. Organomet. Chem.* **2005**, *690*, 2787−2789.

(6) Ewing, W. C.; Carroll, P. J.; Sneddon, L. G. *Inorg. Chem.* **2008**, *47*, 8580−8582.

(7) Ewing, W. C.; Carroll, P. J.; Sneddon, L. G. *Inorg. Chem.* **2010**, *49*, 1983−1994.

(8) *Manipulation of Air Sensitive Compounds,* 2nd ed.; Shriver, D. F., Drezdzon, M. A., Eds.; Wiley: New York, 1986.

(9) Knoth, W. H.; Muetterties, E. L. *J. Inorg. Nucl. Chem.* **1961**, *20*, 66−72.

(10) Muetterties, E. L.; Balthis, J. H.; Chia, Y. T.; Knoth, W. H.; Miller, H. C. *Inorg. Chem.* **1964**, *3*, 444−451.

(11) Ewing, W. C.; Carroll, P. J.; Sneddon, L. G. *Inorg. Chem.* **2011**, *50*, 4054−4064.

(12) Beall, H.; Gaines, D. F. *Inorg. Chem.* **1998**, *37*, 1420−1422.

(13) (a) Li, Y.; Carroll, P. J.; Sneddon, L. G. *Inorg. Chem.* **2008**, *47*, 9193−9202. (b) Kusari, U.; Carroll, P. J.; Sneddon, L. G. *Inorg. Chem.* **2008**, *47*, 9203−9215. (c) Yoon, C. W.; Kusari, U.; Sneddon, L. G. *Inorg. Chem.* **2008**, *47*, 9216−9227. (c) Kusari, U.; Li, Y.; Bradley, M. G.; Sneddon, L. G. *J. Am. Chem. Soc.* **2004**, *126*, 8662−8663. (C) Li, Y.; Kusari, U.; Carroll, P. J.; Bradley, M. G.; Sneddon, L. G. *Pure Appl. Chem.* **2006**, *78*, 1349−1355.

(14) *SAINT,* version 7.68A; Bruker AXS, Inc.: Milwaukee, WI, 2008.

(15) *SHELXTL,* version 6.14; Bruker AXS, Inc.: Milwaukee, WI, 2003.

(16) Frisch, M. J.; Trucks, G. W.; Schlegel, H. B.; Scuseria, G. E.; Robb, M. A.; Cheeseman, J. R.; Scalmani, G.; Barone, V.; Mennucci, B.; Petersson, G. A.; Nakatsuji, H.; Caricato, M.; Li, X.; Hratchian, H. P.; Izmaylov, A. F.; Bloino, J.; Zheng, G.; Sonnenberg, J. L.; Hada, M.; Ehara, M.; Toyota, K.; Fukuda, R.; Hasegawa, J.; Ishida, M.; Nakajima, T.; Honda, Y.; Kitao, O.; Nakai, H.; Vreven, T.; Montgomery, J. A., Jr.; Peralta, J. E.; Ogliaro, F.; Bearpark, M.; Heyd, J. J.; Brothers, E.; Kudin, K. N.; Staroverov, V. N.; Kobayashi, R.; Normand, J.; Raghavachari, K.; Rendell, A.; Burant, J. C.; Iyengar, S. S.; Tomasi, J.; Cossi, M.; Rega, N.; Millam, N. J.; Klene, M.; Knox, J. E.; Cross, J. B.; Bakken, V.; Adamo, C.; Jaramillo, J.; Gomperts, R.; Stratmann, R. E.; Yazyev, O.; Austin, A. J.; Cammi, R.; Pomelli, C.; Ochterski, J. W.; Martin, R. L.; Morokuma, K.; Zakrzewski, V. G.; Voth, G. A.; Salvador, P.; Dannenberg, J. J.; Dapprich, S.; Daniels, A. D.; Farkas, Ö.; Foresman, J. B.; Ortiz, J. V.; Cioslowski, J.; Fox, D. J. *Gaussian 09,* Revision D.01; Gaussian, Inc.: Wallingford, CT, 2009.

(17) Mazighi, K.; Carroll, P. J.; Sneddon, L. G. *Inorg. Chem.* **1993**, *32*, 1963−1969.

(18) (a) Pender, M. J.; Carroll, P. J.; Sneddon, L. G. *J. Am. Chem. Soc.* **2001**, *123*, 12222−12231. (b) Chatterjee, S.; Carroll, P. J.; Sneddon, L. G. *Inorg. Chem.* **2013**, *52*, 9119−9130.

(19) Sprecher, R. F.; Aufderheide, B. E.; Luther, G. W., III; Carter, J. C. *J. Am. Chem. Soc.* **1974**, *96*, 4404−4410.

(20) (a) Bridges, A. N.; Powell, D. R.; Dopke, J. A.; Desper, J. M.; Gaines, D. F. *Inorg. Chem.* **1998**, *37*, 503−509.

(21) (a) Grimes, R. N. *Carboranes,* 2nd ed.; Academic Press: London, U.K., 2011. (b) Heying, T. L.; Ager, J. W., Jr.; Clark, S. L.; Mangold, D. J.; Goldstein, H. L.; Hillman, M.; Polak, R. J.; Szymanski, J. W. *Inorg. Chem.* **1963**, *2*, 1089−1092. (c) Zakharkin, L. I.; Stanko, V. I.; Brattsev, V. A.; Chapovskii, Y. A.; Okhlobystin, O. Y. *Izv. Akad. Nauk SSSR, Ser. Khim.* **1963**, 2238−2239.

(22) Sands, D. S.; Zalkin, A. *Acta Crystallogr.* **1962**, *15*, 410−417.

(23) (a) Kalinin, V. N.; Rys, E. G.; Tyutyunov, A. A.; Starikova, Z. A.; Korlyukov, A. A.; Ol'shevskaya, V. A.; Sung, D. D.; Ponomaryov, A. B.; Petrovskii, P. V.; Hey-Hawkins, E. *Dalton Trans.* **2005**, 903−908. (b) Ol'shevskaya, V. A.; Savchenko, A. N.; Zaitsev, A. V.; Kononova, E. G.; Petrovskii, P. V.; Ramonova, A. A.; Tatarskiy, V. V., Jr.; Uvarov, O. V.; Moisenovich, M. M.; Kalinin, V. N.; Shtil, A. A. *J. Organomet. Chem.* **2009**, *694*, 1632−1637. (c) Ol'shevskaya, V. A.; Dutikova, Y. V.; Tyutyunov, A. A.; Kononova, E. G.; Petrovskii, P. V.; Sung, D. D.; Kalinin, V. N. *Synlett* **2010**, 1265−1267.

(24) (a) Hill, W. E.; Johnson, F. A.; Novak, R. W. *Inorg. Chem.* **1975**, *14*, 1244−1249. (b) Islam, S.; Johnson, F. A.; Hill, W. E.; Silva-Trivino, L. M. *Inorg. Chim. Acta* **1997**, *260*, 99−103.

(25) (a) Plešek, J.; Štíbr, B.; Heřmánek, S. *Collect. Czech. Chem. Commun.* **1966**, *31*, 4744−4745. (b) Gregor, V.; Stuchlík, J. *Collect. Czech. Chem. Commun.* **1973**, *38*, 3623−3626.

(26) Štíbr, B.; Plešek, J.; Heřmánek, S. *Collect. Czech. Chem. Commun.* **1969**, *34*, 194−205.

(27) Bragin, V. I.; Sivaev, I. B.; Bregadze, V. I.; Votinova, N. A. *J. Organomet. Chem.* **2005**, *690*, 2847−2849.

(28) (a) Preetz, W.; Nachtigal, C. *Z. Anorg. Allg. Chem.* **1995**, *621*, 1632−1636. (b) Nachtigal, C.; Preetz, W. *Acta Crystallogr., Sect. C: Cryst. Struct. Commun.* **1996**, *C52*, 453−455.